

## Lanthanide Square Grids

# Tetranuclear Lanthanide(III) Complexes Containing a Square-Grid Core: Synthesis, Structure, and Magnetism

Sourav Biswas,<sup>[a]</sup> Sourav Das,<sup>[b]</sup> Sakiat Hossain,<sup>[a]</sup> Arun Kumar Bar,<sup>[c,d]</sup> Jean-Pascal Sutter,\*<sup>[c,d]</sup> and Vadapalli Chandrasekhar\*<sup>[a,e]</sup>

**Abstract:** The reactions of  $\text{Ln}(\text{NO}_3)_3 \cdot 5\text{H}_2\text{O}$  ( $\text{Ln} = \text{Dy}^{3+}, \text{Tb}^{3+}, \text{Ho}^{3+}, \text{Er}^{3+}$ ) and a multidentate flexible ligand, (*E*)- $N'$ -[2-hydroxy-3-(hydroxymethyl)-5-methylbenzylidene]-6-(hydroxymethyl)picolinohydrazide ( $\text{LH}_4$ ), in the presence of  $\text{Et}_3\text{N}$  in a 1:1:3 molar ratio afforded a series of complexes  $[\text{Ln}_4(\text{LH}_2)_4(\mu_2\text{-OH})_4] \cdot x\text{CH}_3\text{OH} \cdot y\text{H}_2\text{O}$  ( $\text{Dy}^{3+}, x = 2, y = 2; \text{Tb}^{3+}, x = 4, y = 5; \text{Ho}^{3+}, x = 0, y = 13; \text{Er}^{3+}, x = 4, y = 6$ ). X-ray diffraction analysis revealed that all the complexes are neutral and possess a distorted  $[2 \times 2]$  square-grid core  $[\text{Ln}_4(\mu_2\text{-O})_4(\mu_2\text{-OH})_4]$  anchored by the concerted coordination of four doubly deprotonated ligands,

( $\text{LH}_2$ ) $^{2-}$ , and four  $\mu_2\text{-OH}$  groups. All the Ln centers adopt a distorted triangular dodecahedral coordination geometry. An ac magnetic susceptibility study revealed undulations of the out-of-phase ( $\chi_M''$ ) component above 2 K for **1** with a quantum tunnelling of magnetization tail at zero dc field. Surprisingly, a field-induced temperature dependence of the ac frequencies at which the  $\chi_M''$  maxima occur implies that the slow relaxation is a result of a mixed contribution from more than one  $\text{Dy}^{3+}$  center.

## Introduction

Since the seminal finding that the dodecanuclear complex  $[\text{Mn}_{12}\text{O}_{12}(\text{OAc})_{16}(\text{H}_2\text{O})_4] \cdot 2\text{HOAc} \cdot 4\text{H}_2\text{O}$ <sup>[1]</sup> acts as a single-molecule magnet, tremendous efforts are being made in the field of molecular magnets to improve their characteristics. The excitement and interest in this field have arisen for several reasons. For example, at a fundamental level, these compounds and the phenomenon they exhibit are of relevance to physicists interested in quantum phenomenon such as quantum computation<sup>[2]</sup> and quantum tunneling.<sup>[3]</sup> Moreover, these systems are projected to have several applications ranging from high-density information storage<sup>[3c,4]</sup> to magnetic refrigeration.<sup>[5]</sup>

Molecular magnets, such as single-molecule magnets (SMMs), single-ion magnets (SIMs), and single-chain magnets (SCMs), are characterized by a slow relaxation of magnetization

below a certain temperature (called the blocking temperature,  $T_B$ ). The super-paramagnet-like behavior of such systems seems to arise from a large ground-state spin ( $S$ ) in combination with a high uniaxial magnetic anisotropy ( $D$ ) leading to an energy barrier ( $U$ ) to magnetization reversal.  $U$  can be defined as  $|D|S^2$  for integer values of  $S$  and  $|D|(S^2 - 1/4)$  for half-integer values of  $S$ .<sup>[1b,6]</sup> With this in mind, several strategies have been adopted by synthetic chemists to assemble these materials. These include the preparation of polynuclear 3d,<sup>[7]</sup> 3d/4f,<sup>[8]</sup> and 4f compounds.<sup>[9]</sup> Among such systems, the most fascinating behaviors are exhibited by Ln-based complexes, particularly those involving  $\text{Dy}^{3+}$ ,  $\text{Tb}^{3+}$ ,  $\text{Ho}^{3+}$ , and  $\text{Er}^{3+}$ .<sup>[10]</sup> These ions have a large  $D$  parameter because of their diffuse valence orbitals and consequent significant unquenched orbital angular momentum, which renders strong spin-orbital coupling (SOC). Recent reports describing systems such as  $[\text{Dy}_4\text{K}_2\text{O}(\text{OtBu})_{12}]$ ,<sup>[11]</sup>  $[\text{Dy}_5\text{O}(\text{OiPr})_{13}]$ ,<sup>[12]</sup>  $[\text{Cp}_2\text{Dy}(\text{thf})(\mu\text{-Cl})]$ <sup>[13]</sup> ( $\text{Cp} = \text{cyclopentadiene}$ ), and  $[(\text{Cp}^*\text{2Ln})_2(\mu\text{-bpym})]^+$  ( $\text{Cp}^* = \text{pentamethylcyclopentadienyl}; \text{bpym} = 2,2'\text{-bipyrimidine}; \text{Ln} = \text{Gd}^{3+}, \text{Tb}^{3+}$ )<sup>[14]</sup> have motivated synthetic chemists to prepare new families of lanthanide complexes with the hope of achieving a new family of SMMs.

We have been working for some time on 3d/4f<sup>[8i,8m,15]</sup> and 4f<sup>[16]</sup> complexes. Interesting SMM behavior has been observed, in particular, in the  $\text{Ln}_4$  family of complexes  $[(\text{LH})_2\text{Ln}_4] \cdot (\mu_2\text{-O})_4(\text{H}_2\text{O})_8$  ( $\text{Ln} = \text{Dy}^{3+}, \text{Ho}^{3+}; \text{LH}_3 = (6\text{-hydroxymethyl})\text{-}N'\text{-}[(8\text{-hydroxyquinolin-2-yl})\text{methylene}]picolinohydrazide$ ),<sup>[16a]</sup> which possess rhombus-shaped geometry (Scheme 1, a). Notably, we observed two relaxation time constants in such complexes and these were attributed to differences in geometry at the  $\text{Dy}^{3+}$  ions. In addition, we also prepared  $\text{Ln}_4$  complexes containing two dinuclear sub-units (Scheme 1, b).<sup>[17]</sup> Very recently we also

[a] Department of Chemistry, Indian Institute of Technology Kanpur, Kanpur 208016, India  
E-mail: vc@iitk.ac.in  
vc@niser.ac.in

[b] Department of Chemistry, Institute of Infrastructure Technology Research and Management, Near Khokhara Circle, Maninagar East, Ahmedabad 380026, India

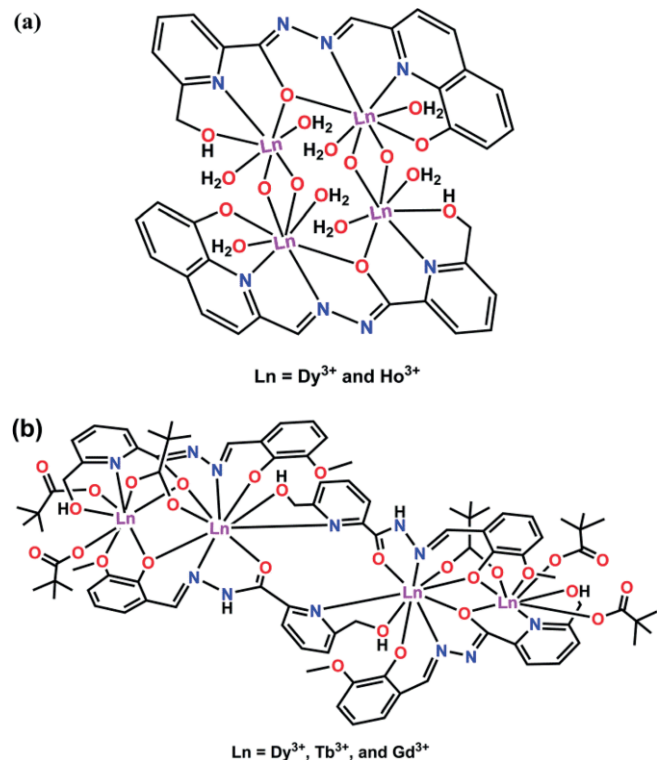
[c] CNRS, LCC (Laboratoire de Chimie de Coordination), 205 route de Narbonne, 31077 Toulouse, France  
E-mail: jean-pascal.sutter@lcc-toulouse.fr

[d] Université de Toulouse, UPS, INPT, LCC, 31077 Toulouse Cedex 4, France

[e] National Institute of Science Education and Research, Jatni Campus, PO: Bhimpur-Padanpur, Bhubaneswar 752050, Orissa, India

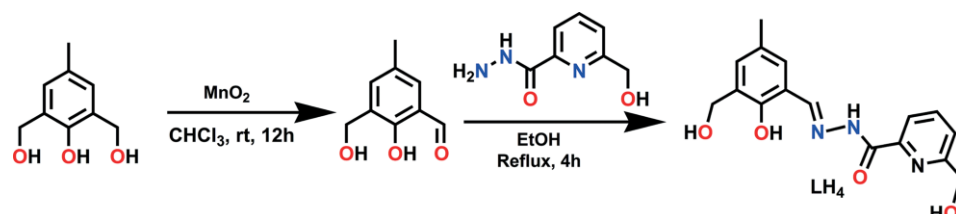
Supporting information for this article is available on the WWW under <http://dx.doi.org/10.1002/ejic.201600744>.

reported planar square-grid complexes, but none of these showed SMM behavior.<sup>[17,18]</sup> These results as well as the fact that planar square-shaped  $\text{Ln}_4$  cores are quite rare motivated us to examine whether new synthetic strategies could lead to new SMM families of tetranuclear lanthanide complexes containing planar (square) cores.



Scheme 1. a) Rhombus-shaped  $\text{Ln}_4$  complexes.<sup>[16a]</sup> b)  $\text{Ln}_4$  complexes in which both the keto and enol forms of the ligand are involved in binding.<sup>[17]</sup>

We report herein a new multidentate aroyl hydrazone ligand, (*E*)-*N'*-[2-hydroxy-3-(hydroxymethyl)-5-methylbenzylidene]-6-(hydroxymethyl)picolinohydrazide ( $\text{LH}_4$ ; see Scheme 2), which, upon reaction with  $\text{Ln}(\text{NO}_3)_3 \cdot 5\text{H}_2\text{O}$  ( $\text{Ln} = \text{Dy}^{3+}, \text{Tb}^{3+}, \text{Ho}^{3+}, \text{Er}^{3+}$ ) afforded a series of distorted square-grid complexes  $[\text{Ln}_4(\text{LH}_4)_4(\mu_2-\text{OH})_4] \cdot x\text{CH}_3\text{OH} \cdot y\text{H}_2\text{O}$  [ $\text{Dy}^{3+}$ ,  $x = 2, y = 2$  (**1**);  $\text{Tb}^{3+}$ ,  $x = 4, y = 5$  (**2**);  $\text{Ho}^{3+}$ ,  $x = 0, y = 13$  (**3**);  $\text{Er}^{3+}$ ,  $x = 4, y = 6$  (**4**)]. The synthesis, structures, and magnetic behavior of these complexes are discussed herein.



Scheme 2. Synthesis of  $\text{LH}_4$ .

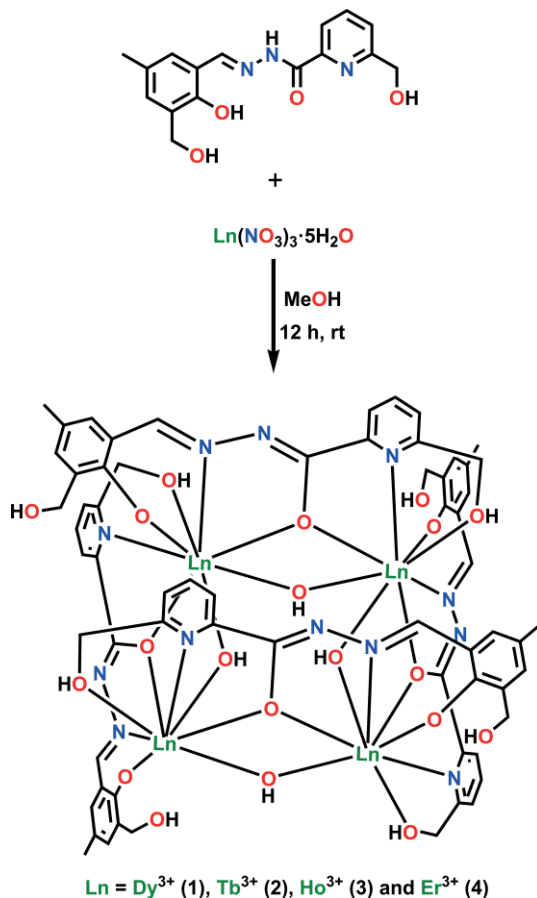
## Results and Discussion

Aroyl hydrazone ligands are proving to be quite versatile in affording polynuclear lanthanide complexes.<sup>[19]</sup> The features that can be modulated in this ligand system are the compartmental coordination pockets, keto-enol tautomerism, which can allow either the keto or the enolate form to be involved in binding, the hydrazone nitrogen atoms and other coordinating groups that can be incorporated at the periphery of the ligand. In addition, such ligands seem to possess coordination flexibility to suit the needs of the interacting metal ions. In previous work we exploited these concepts to construct two families of  $\text{Ln}_4$  assemblies: 1) rhombus-shaped complexes, in which the enolate form of the ligand (6-hydroxymethyl)-*N'*-(8-hydroxyquinolin-2-yl)methylene]picolinohydrazide is involved in binding (Scheme 1, a) and 2) a tetranuclear complex containing two dinuclear sub-units (Scheme 1, b). In the latter case, the ligand [*N'*-(2-hydroxy-3-methoxybenzylidene)-6-(hydroxymethyl)picolinohydrazide] is involved in linking the two dinuclear units by involving both the keto and enol forms of the ligand, a feature that also attests to the conformational flexibility of such ligands.<sup>[17]</sup>

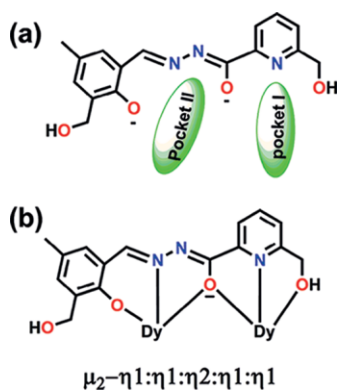
It is worth mentioning that four homometallic  $\text{Ln}_4$  [2 × 2] square-grid complexes have been reported in the literature<sup>[18,20]</sup> that exploit similar design features. With this in mind, we synthesized a new aroyl hydrazone based ligand, (*E*)-*N'*-[2-hydroxy-3-(hydroxymethyl)-5-methylbenzylidene]-6-(hydroxymethyl)picolinohydrazide ( $\text{LH}_4$ ), following a two-step synthetic protocol (Scheme 2). The multidentate ligand  $\text{LH}_4$  consists of divergent coordinating sites such as a pyridyl and imino N atom, which can effectively bind to lanthanide centers, a hydrazone oxygen, which can either undergo enolization or retain its keto form, a phenolic OH and a pendant  $\text{CH}_2\text{OH}$ , which can proliferate the nuclearity of the lanthanide complexes depending upon the degree of their deprotonation.

The reaction of  $\text{Ln}(\text{NO}_3)_3 \cdot 5\text{H}_2\text{O}$  and  $\text{LH}_4$  in methanol in a 1:1 stoichiometry in the presence of 3 equiv. of triethylamine led to the formation of neutral homometallic  $\text{Ln}_4$  complexes  $[\text{Dy}_4(\text{LH}_4)_4(\mu_2-\text{OH})_4] \cdot 2\text{CH}_3\text{OH} \cdot 2\text{H}_2\text{O}$  (**1**),  $[\text{Tb}_4(\text{LH}_4)_4(\mu_2-\text{OH})_4] \cdot 4\text{CH}_3\text{OH} \cdot 5\text{H}_2\text{O}$  (**2**),  $[\text{Ho}_4(\text{LH}_4)_4(\mu_2-\text{OH})_4] \cdot 13\text{H}_2\text{O}$  (**3**), and  $[\text{Er}_4(\text{LH}_4)_4(\mu_2-\text{OH})_4] \cdot 4\text{CH}_3\text{OH} \cdot 6\text{H}_2\text{O}$  (**4**; Scheme 3). The organization of the coordinating sites in the enolized form of the ligand leads to two effective ONO coordination pockets each of which holds one lanthanide center (Scheme 4, a).

To investigate the structural integrity of the complexes in solution, we carried out ESI-MS analyses (see the Exp. Sect.). The appearance of prominent peaks at around 1000.60, 979.07,



Scheme 3. Synthesis of tetrametallic  $\text{Ln}_4$  complexes 1–4.



Scheme 4. a) Two coordinating pockets of  $[\text{LH}_2]^{2-}$  in its enolized form and b) binding mode of the ligand in its enolized form with  $\text{Dy}^{3+}$  ions.

996.08, and 1010.10 can be attributed to the dicationic species  $[\text{C}_{64}\text{H}_{62}\text{Dy}_4\text{N}_{12}\text{O}_{18} + 2\text{MeOH}]^{2+}$ ,  $[\text{C}_{64}\text{H}_{62}\text{Tb}_4\text{N}_{12}\text{O}_{18} + 2\text{H}_2\text{O}]^{2+}$ ,  $[\text{C}_{64}\text{H}_{62}\text{Ho}_4\text{N}_{12}\text{O}_{18} + \text{H}_2\text{O} + \text{MeOH}]^{2+}$ , and  $[\text{C}_{64}\text{H}_{62}\text{Er}_4\text{N}_{12}\text{O}_{18} + 2\text{MeOH}]^{2+}$ , respectively, due to the loss of two OH groups from each of the complexes. These results suggest the existence of tetranuclear units in solution for all the complexes. The ESI-MS spectrum of complex 1 is shown in Figure 1 as a representative example, those of 2–4 are given in the Supporting Information (Figures S1–S3).

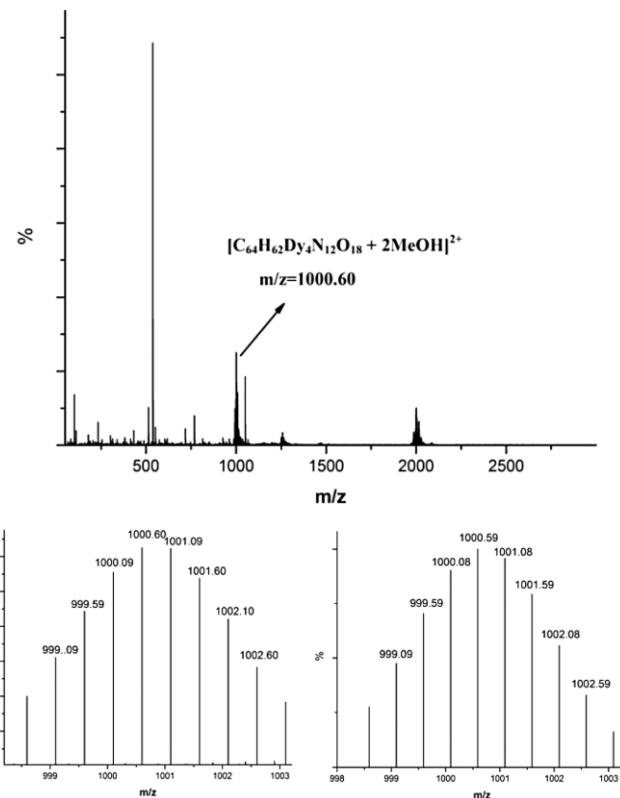


Figure 1. Full-range ESI-MS spectrum of complex 1 (top). Experimental (bottom left) and simulated (bottom right) isotopic distribution of the ionized species  $[\text{C}_{64}\text{H}_{62}\text{Dy}_4\text{N}_{12}\text{O}_{18} + 2\text{MeOH}]^{2+}$ .

### X-ray Crystal Structures of 1–4

Complexes 1–4 crystallize in the triclinic system with space group  $P\bar{1}$ . All these complexes are neutral and possess the same square-grid structural topology (Figure 2). In view of this, only the structure of 1 is discussed as a representative example. The perspective view of the molecular structure 1 is depicted in Figure 2, and the structures of 2–4 are given in the Supporting Information (Figures S4–S6). Selected bond lengths and angles of 1 are given in Table 1 and those of 2–4 are given in Tables S1–S3.

The formation of the tetranuclear complexes can be described in the following way. Each ligand in its dianionic form ( $\text{LH}_2^{2-}$ ) adopts a  $\mu_2-\eta^1: \eta^1: \eta^2: \eta^1$  coordination mode (Scheme 4, b) to accommodate two  $\text{Dy}^{3+}$  centers in its two tridentate coordinating pockets. Importantly, the ligands coordinate solely in their enol form.

The cumulative coordinative action of four enolized dianionic ( $\text{LH}_2^{2-}$ ) ligands leads to the construction of the square-grid core that incorporates  $\text{Dy}^{3+}$  ions at the corners. In addition to the binding provided by ( $\text{LH}_2^{2-}$ ), the four  $\text{Dy}^{3+}$  centers are also tightly held together by four  $\mu\text{-OH}$  groups, which contribute additional strength to the cluster. Notably, the ligands involved in holding each pair of this square grid project upwards in a slightly tilted manner with respect to each other such that the steric congestion is minimized.

Table 1. Selected bond lengths and bond angles for **1**.

Bond lengths [Å] around Dy <sup>3+</sup>	Bond angles [°] around Dy <sup>3+</sup>				
Dy1–O9	2.167(7)	O7–Dy1–N6	143.8(2)	O10–Dy2–Dy4	95.6(2)
Dy1–O1	2.271(6)	O12–Dy1–N6	81.9(2)	O6–Dy2–Dy4	104.87(15)
Dy1–O6	2.318(7)	O17–Dy1–N6	134.1(2)	O17–Dy2–Dy4	74.26(14)
Dy1–O7	2.380(6)	O9–Dy1–N1	74.4(3)	N4–Dy2–Dy4	109.57(17)
Dy1–O12	2.408(6)	O1–Dy1–N1	132.3(2)	N12–Dy2–Dy4	97.7(3)
Dy1–O17	2.491(7)	O6–Dy1–N1	131.4(3)	O20–Dy2–Dy1	83.8(2)
Dy1–N6	2.522(8)	O7–Dy1–N1	64.2(2)	O4–Dy2–Dy1	76.51(16)
Dy1–N1	2.535(8)	O12–Dy1–N1	63.4(2)	O5–Dy2–Dy1	112.6(2)
Dy1–Dy3	3.8231(7)	O17–Dy1–N1	79.9(2)	O10–Dy2–Dy1	162.6(2)
Dy1–Dy2	3.9271(8)	N6–Dy1–N1	131.1(2)	O6–Dy2–Dy1	32.83(16)
Dy2–O20	2.204(7)	O9–Dy1–Dy3	101.47(17)	O17–Dy2–Dy1	37.45(16)
Dy2–O4	2.286(6)	O1–Dy1–Dy3	33.98(16)	N4–Dy2–Dy1	97.5(2)
Dy2–O5	2.352(7)	O6–Dy1–Dy3	106.74(15)	N12–Dy2–Dy1	115.1(3)
Dy2–O10	2.358(8)	O7–Dy1–Dy3	35.39(15)	Dy4–Dy2–Dy1	89.836(15)
Dy2–O6	2.384(7)	O12–Dy1–Dy3	154.93(17)	O11–Dy3–O1	157.2(2)
Dy2–O17	2.411(7)	O17–Dy1–Dy3	71.98(14)	O11–Dy3–O7	134.6(2)
Dy2–N4	2.483(9)	N6–Dy1–Dy3	122.58(16)	O1–Dy3–O7	68.2(2)
Dy2–N12	2.560(9)	N1–Dy1–Dy3	98.56(17)	O11–Dy3–O8	80.8(2)
Dy2–Dy4	3.8375(8)	O9–Dy1–Dy2	168.56(17)	O1–Dy3–O8	79.1(2)
Dy3–O11	2.192(7)	O1–Dy1–Dy2	82.60(18)	O7–Dy3–O8	136.7(2)
Dy3–O1	2.319(6)	O6–Dy1–Dy2	33.90(16)	O11–Dy3–O3	93.7(3)
Dy3–O7	2.333(6)	O7–Dy1–Dy2	107.14(18)	O1–Dy3–O3	89.5(2)
Dy3–O8	2.344(7)	O12–Dy1–Dy2	81.29(18)	O7–Dy3–O3	81.8(3)
Dy3–O3	2.363(7)	O17–Dy1–Dy2	36.06(16)	O8–Dy3–O3	70.0(2)
Dy3–O16	2.397(8)	N6–Dy1–Dy2	98.07(19)	O11–Dy3–O16	91.3(3)
Dy3–N7	2.497(8)	N1–Dy1–Dy2	108.6(2)	O1–Dy3–O16	93.2(3)
Dy3–N3	2.544(8)	Dy3–Dy1–Dy2	89.140(14)	O7–Dy3–O16	81.2(2)
Dy3–Dy4	3.8684(8)	O20–Dy2–O4	155.9(3)	O8–Dy3–O16	129.4(2)
Dy4–O18	2.231(8)	O20–Dy2–O5	135.3(3)	O3–Dy3–O16	160.5(2)
Dy4–O4	2.248(6)	O4–Dy2–O5	66.6(2)	O11–Dy3–N7	76.3(3)
Dy4–O8	2.337(7)	O20–Dy2–O10	94.9(3)	O1–Dy3–N7	85.5(2)
Dy4–O5	2.356(7)	O4–Dy2–O10	99.7(3)	O7–Dy3–N7	135.4(3)
Dy4–O3	2.393(8)	O5–Dy2–O10	80.4(3)	O8–Dy3–N7	65.3(3)
Dy4–O19	2.426(7)	O20–Dy2–O6	77.6(3)	O3–Dy3–N7	135.2(3)
Dy4–N10	2.516(10)	O4–Dy2–O6	78.3(2)	O16–Dy3–N7	64.3(3)
Dy4–N9	2.573(9)	O5–Dy2–O6	137.7(2)	O11–Dy3–N3	71.2(2)
		O10–Dy2–O6	129.9(3)	O1–Dy3–N3	131.6(2)
		O20–Dy2–O17	91.7(3)	O7–Dy3–N3	63.6(2)
Bond angles [°] around Dy <sup>3+</sup>	O4–Dy2–O17	81.1(2)	O8–Dy3–N3	137.1(3)	
	O5–Dy2–O17	81.3(3)	O3–Dy3–N3	79.8(3)	
O9–Dy1–O1	103.8(3)	O10–Dy2–O17	159.7(3)	O16–Dy3–N3	84.0(3)
O9–Dy1–O6	136.3(2)	O6–Dy2–O17	70.3(2)	N7–Dy3–N3	133.5(3)
O1–Dy1–O6	83.4(2)	O20–Dy2–N4	86.4(3)	O11–Dy3–Dy1	168.08(18)
O9–Dy1–O7	84.2(2)	O4–Dy2–N4	82.6(2)	O1–Dy3–Dy1	33.19(15)
O1–Dy1–O7	68.2(2)	O5–Dy2–N4	128.8(3)	O7–Dy3–Dy1	36.20(16)
O6–Dy1–O7	136.2(2)	O10–Dy2–N4	65.1(3)	O8–Dy3–Dy1	104.15(16)
O9–Dy1–O12	90.6(3)	O6–Dy2–N4	65.1(3)	O3–Dy3–Dy1	78.18(16)
O1–Dy1–O12	160.9(2)	O17–Dy2–N4	134.6(3)	O16–Dy3–Dy1	93.65(17)
O6–Dy1–O12	77.6(2)	O20–Dy2–N12	71.6(3)	N7–Dy3–Dy1	115.61(19)
O7–Dy1–O12	126.7(2)	O4–Dy2–N12	129.6(3)	N3–Dy3–Dy1	98.56(17)
O9–Dy1–O17	152.2(2)	O5–Dy2–N12	63.8(3)	O11–Dy3–Dy4	87.4(2)
O1–Dy1–O17	85.9(2)	O10–Dy2–N12	80.6(3)	O1–Dy3–Dy4	82.08(17)
O6–Dy1–O17	69.9(2)	O6–Dy2–N12	138.5(3)	O7–Dy3–Dy4	111.15(18)
O7–Dy1–O17	75.2(2)	O17–Dy2–N12	83.3(3)	O8–Dy3–Dy4	34.22(16)
O12–Dy1–O17	87.1(2)	N4–Dy2–N12	137.4(3)	O3–Dy3–Dy4	35.85(18)
O9–Dy1–N6	72.7(3)	O20–Dy2–Dy4	163.5(2)	O16–Dy3–Dy4	163.54(17)
O1–Dy1–N6	90.4(2)	O4–Dy2–Dy4	31.88(15)	N7–Dy3–Dy4	99.5(2)
O6–Dy1–N6	64.2(2)	O5–Dy2–Dy4	35.44(17)	N3–Dy3–Dy4	111.0(2)

The  $[\text{Dy}_4(\mu_2\text{-O})_4(\mu_2\text{-OH})_4]$  core consists of four four-membered  $\text{Dy}_2\text{O}_2$  sub-units (Figure 2, bottom), analogous to the cores reported previously by us<sup>[18]</sup> as well as Murugesu,<sup>[20c]</sup> Thompson,<sup>[20b]</sup> and Tang<sup>[20a]</sup> and their co-workers. Each of the  $\text{Dy}^{3+}$  centers possesses a distorted trigonal dodecahedron coor-

dination geometry and are coordinated by six oxygen and two nitrogen atoms (Figure 3, top). In spite of having the same coordination environment around the  $\text{Dy}^{3+}$  ions, all the  $\text{Dy}-\text{N}_{\text{py}}$  distances fall in the range 2.476–2.539 Å whereas the  $\text{Dy}-\text{O}_{\text{phen}}$  distances range from 2.164–2.238 Å.

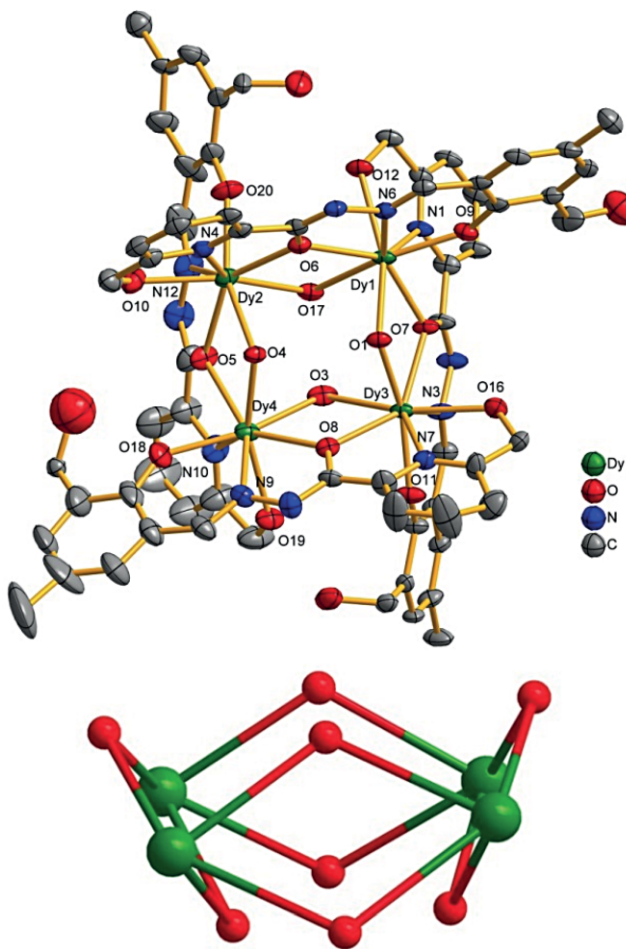


Figure 2. Top: ORTEP diagram of **1**. Thermal ellipsoids are drawn at the 40 % probability level. Hydrogen atoms, solvent molecules and the disordered parts of the ligands have been omitted for clarity. Bottom: [2 × 2] square-grid core of complex **1**.

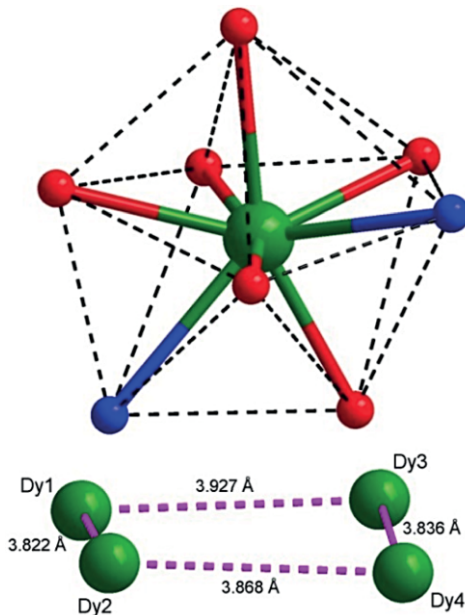
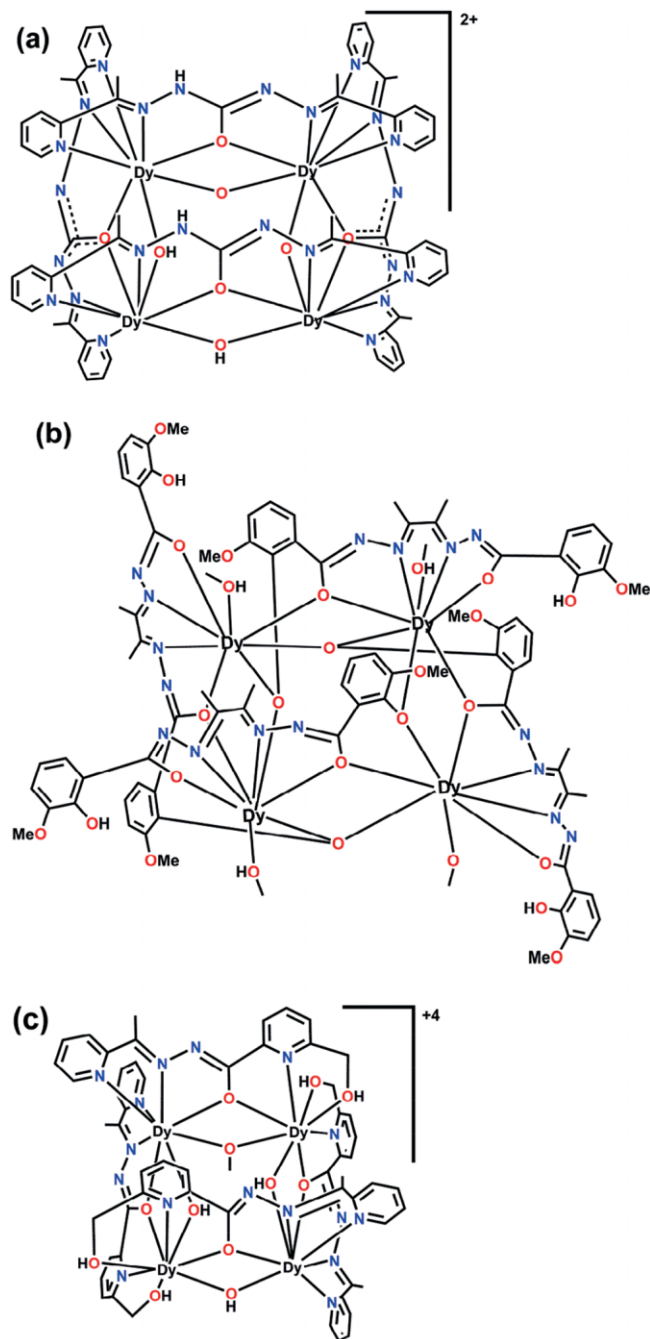


Figure 3. Distorted triangular dodecahedral geometry around the Dy<sup>3+</sup> ion (top) and the distorted square-grid core highlighting the distances between consecutive metal centers (bottom) of **1**.

The Dy-μ-OH-Dy bond angles vary over a wider range (108.6–115.9°) than the Dy-μ-O<sub>hydrazone</sub>-Dy bond angles (109.1–111.5°), which may account for the slight distortion in the square grid. In addition to this, the Dy-Dy distances in the square grid lie in the range 3.82–3.93 Å (Figure 3, bottom).

Precedents involving Ln<sub>4</sub> complexes containing a square-grid geometry (Scheme 5) involving mainly symmetric dihydrazide ligands have been reported in the literature.<sup>[18,20a,20b]</sup> We have explored aryl hydrazone ligands.<sup>[19a,19b]</sup> The structural features of three known tetranuclear Dy<sup>3+</sup> square-grid complexes are summarized in Table 2 and compared with those of complex **1**. Of the three literature precedents, one has four μ-OH ligands,



Scheme 5. Square-grid Dy<sub>4</sub> complexes reported in the literature.<sup>[18,20a,20b]</sup>

Table 2. Comparison of bond lengths and angles in the square-grid core of  $\text{Ln}_4$  complexes.

Ligand	$\text{Dy}-\text{N}_{\text{py}} \text{ [\AA]}$	$\text{Dy}-\text{O}_{\text{phen}} \text{ [\AA]}$	$\text{Dy}-\text{N}_{\text{immino}} \text{ [\AA]}$	$\text{Dy}-\text{Dy} \text{ [\AA]}$	$\text{Dy}-\text{O}-\text{Dy} \text{ [°]}$
$[\text{Dy}_4(\text{HL})_4(\text{MeOH})_4]^{[20b]}$ $\text{LH}_4 = N',N''-(\text{butane-2,3-diylidene})\text{bis}(2-\text{hydroxy-3-methoxybenzohydrazide})$		2.27–2.37	2.45–2.49	3.82–3.87	107.2–109.9
$[\text{Dy}_4(\text{L})_4(\text{OH})_4]\text{Cl}_2^{[21]}$ $\text{LH}_2 = 2-[1-(\text{pyridin-2-yl})\text{ethylidene}] \text{hydrazinyl hydrazide}$	2.540–2.56		2.52–2.53	3.76–3.79	107.3–108.4
$[\text{Dy}_4(\text{LH})_4(\mu_2-\text{OH})_3(\mu_2-\text{OMe})_1]\text{4NO}_3^{[19]}$ $\text{LH}_2 = 6-(\text{hydroxymethyl})-\text{N}'-[1-(\text{pyridin-2-yl})\text{ethylidene}] \text{picolinohydrazide}$	2.48–2.576		2.47–2.59	3.78–3.82	107.2–110.8
$[\text{Dy}_4(\text{LH}_2)_4(\mu_2-\text{OH})_4]$ (1) $\text{LH}_4 = (\text{E})-\text{N}'-[2-\text{hydroxy-3-(hydroxymethyl)-5-methylbenzylidene}-6-(hydroxymethyl)] \text{picolinohydrazide}$ (this work)	2.47–2.53	2.16–2.23	2.51–2.56	3.82–3.92	109.1–111.5

similarly to the present instance,<sup>[20c]</sup> another has three  $\mu$ -OH and one  $\mu$ -OMe ligand,<sup>[18]</sup> and in the last example,<sup>[20a]</sup> phenolate oxygen atoms serve the purpose of bridging the lanthanide ions (Scheme 5, b). Also, the distortion observed in the square grid in complex **1** is larger than in two of the literature precedents,<sup>[20a,20c]</sup> (Table 2).

## Magnetic Studies

The temperature dependence of  $\chi_M T$  ( $\chi_M$  is the molar susceptibility) and the magnetization versus field at 2 K have been investigated for **1–4** (see Figure S7 in the Supporting Information). All exhibit very similar behavior, therefore only the Dy<sup>3+</sup> homologue **1** is described in detail below (further information can be found in Figures S8–S10 in the Supporting Information). For **1**, the value for  $\chi_M T$  at 300 K was found to be 56.0 cm<sup>3</sup> K mol<sup>-1</sup> (see Figure S7, left), in good agreement with the expected contribution of four Dy<sup>3+</sup> ions (i.e., 56.7 cm<sup>3</sup> K mol<sup>-1</sup>) in the absence of exchange interactions. This value diminishes as  $T$  is lowered to reach 43.9 cm<sup>3</sup> K mol<sup>-1</sup> at 2 K, behavior that can be ascribed mainly to the crystal field effect on Dy<sup>3+</sup>.<sup>[21]</sup> The rather large  $\chi_M T$  observed at 2 K is indicative of very weak, if any, exchange interactions between the Ln<sup>3+</sup> centers. Similar behavior was found for complexes **2–4** (see Figure S7).

The field dependence of the magnetization observed at low  $T$  for all complexes (see Figure S7, right) is characterized by a rapid increase at weak fields followed by a more gradual but steady increase at higher fields. The values reached for a field of 5 T at 2 K are 20.9  $\mu_B$  (**1**), 18.2  $\mu_B$  (**2**), 20.1  $\mu_B$  (**3**), and 17.5  $\mu_B$  (**4**).

The slow dynamics of the relaxation of magnetization were examined for all complexes by ac susceptibility measurements. An out-of-phase ( $\chi_M''$ ) signal was found for **1** below 15 K in the absence of an applied dc field, but the tail characteristic of quantum tunneling of magnetization (QTM) was observed. This QTM was reduced in the presence of a dc magnetic field, but the shape of the  $\chi_M''$  versus  $T$  curve broadened as  $H_{\text{DC}}$  increased (see Figure S11 in the Supporting Information). The signal obtained at  $H_{\text{DC}} = 3$  kOe appears to be the best compromise between reduced QTM and peak broadening, and therefore a full data set for different frequencies was collected with this applied field.

Figure 4 shows the plots of  $\chi_M''$  versus  $T$  for frequencies between 28 and 1500 Hz and  $\chi_M''$  versus frequency for temperatures between 2 and 6 K. Clearly, these plots are not consistent with the behavior expected for an SMM. In the former, rather than a displacement of the maximum of  $\chi_M''$  to a higher  $T$  with increasing frequency, the shape of the  $\chi_M''$  versus  $T$  curves change. In particular, the undulations seen in the curves obtained at 28, 50, and 100 Hz suggest that the overall  $\chi_M''$  signal results from several contributions with similar temperature maxima.

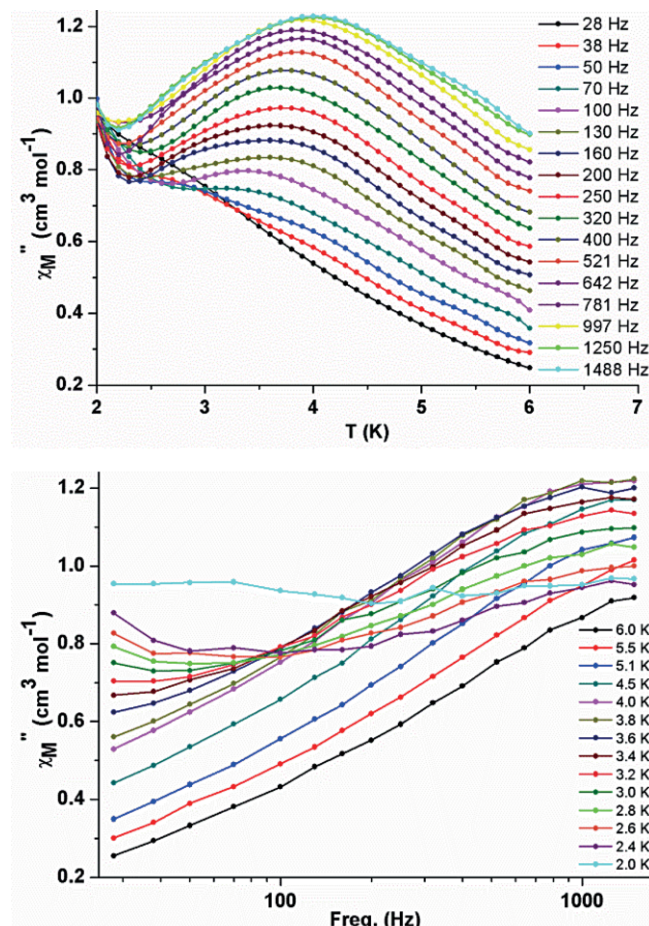


Figure 4.  $\chi_M''$  vs.  $T$  plots for different frequencies (top) and  $\chi_M''$  vs. frequency for temperatures between 2.4 and 5.9 K (bottom). The susceptibility data were recorded at  $H_{\text{DC}} = 3$  kOe.

For frequencies of 200 Hz and above, this leads to a broad signal, the intensity of which increases with frequency and the maximum is slightly shifted to higher  $T$ . Such behavior could be rationalized by considering independent contributions from more than one (if not four) of the crystallographically independent  $Dy^{3+}$  centers<sup>[16a,17]</sup> with  $\chi_M''$  maxima occurring at a similar temperature, hence resulting in the overlap of individual signals. In no case can this shift in  $T$  be considered as a shift of a given maximum, as is usually seen for SMMs. This is supported by the plot of  $\chi_M''$  versus frequency (Figure 4, bottom), which does not show the displacement of the maximum towards higher frequency as a function of temperature, at least not in the frequency domain (<1500 Hz) that we can investigate. In such a situation, the extraction of any information regarding the energy barrier for spin reversal does not make sense. Ab initio calculations in combination with spectroscopic investigations could provide an insight into the actual relaxation processes operating in this complex.<sup>[22]</sup> However, the overall modest performances exhibited by the complex do not justify such demanding investigations, moreover poly-Ln complexes showing independent multi-relaxation features are well documented.<sup>[10a,10f,10j,16a,17,22,23]</sup>

For the  $Tb_4$  (**2**) and  $Ho_4$  (**3**) derivatives, the ac susceptibility data did not show a signal deviating from zero for  $\chi_M''$  even when a dc field was applied. For the  $Er_4$  complex (**4**), only the onset of the signal for  $\chi_M''$  was found above 2 K, even in the presence of an applied dc field (see Figure S10 in the Supporting Information).

## Conclusions

We have reported herein the synthesis and structural and magnetic characterization of homometallic tetrานuclear lanthanide ( $Ln_4$ ) complexes [ $Ln = Dy^{3+}$  (**1**),  $Tb^{3+}$  (**2**),  $Ho^{3+}$  (**3**),  $Er^{3+}$  (**4**)]. The distorted [2 × 2] square-grid core was assembled by employing a multidentate aryl hydrazone based ligand that coordinates exclusively in the enol form to hold one lanthanide center in each of the two distinct pockets with the core further strengthened by four  $\mu_2$ -OH ligands. Regarding the magnetic behavior of these complexes and especially the ac magnetic susceptibility, slow relaxation of the magnetization was found for the  $Dy^{3+}$  and  $Er^{3+}$  derivatives at low temperature. However, the out-of-phase component suggests that several magnetic sites contribute concomitantly to the observed signal. Such behavior is often found in polynuclear  $Ln^{3+}$  compounds and results from the structural differences at the  $Ln^{3+}$  centers that modulate the individual SMM characteristics. In the present case, all four independent  $Ln^{3+}$  have similar coordination spheres and therefore are likely to exhibit similar characteristics for the relaxation dynamics of their magnetization. As a result, their magnetic signatures occur within a very narrow temperature domain. An open question remains the possible role of exchange coupling; unfortunately it proved impossible to obtain the related  $Gd^{3+}$  derivative that would have revealed its occurrence in these compounds.

## Experimental Section

Solvents and other general reagents used in this work were purified according to standard procedures.<sup>[24]</sup> Pyridine-2,6-dicarboxylic acid, sodium borohydride, 2,6-bis(hydroxymethyl)-4-methylphenol, activated manganese(IV) dioxide ( $MnO_2$ ),  $Dy(NO_3)_3 \cdot 5H_2O$ ,  $Tb(NO_3)_3 \cdot 5H_2O$ ,  $Ho(NO_3)_3 \cdot 5H_2O$ , and  $Er(NO_3)_3 \cdot 5H_2O$  were obtained from Sigma Aldrich Chemical Co. and were used as received. Hydrazine hydrate (80 %) and sodium sulfate (anhydrous) were obtained from SD Fine Chemicals, Mumbai, India, and were used as such. Methyl 6-(hydroxymethyl)picolinate, 6-(hydroxymethyl)picolino-hydrazide,<sup>[17]</sup> and 6-formyl-2-(hydroxymethyl)-4-methylphenol<sup>[8h]</sup> were prepared according to literature procedures.

**Instrumentation:** Melting points were measured with a JSGW melting-point apparatus. IR spectra were recorded as KBr pellets with a Bruker Vector 22 FT IR spectrophotometer operating at 400–4000  $cm^{-1}$ . Elemental analyses of the compounds were performed with a Thermoquest CE CHNS-O instrument, EA/110 model. Electrospray ionization mass spectrometry (ESI-MS) was carried out in methanol with a Micromass Quattro II triple quadrupole mass spectrometer with an applied cone voltage of 5 V and a capillary voltage of 3.5 kV.  $^1H$  NMR spectra were recorded in  $CD_3OD$  solutions with a JEOL JNM LAMBDA 400 spectrometer operating at 500 MHz. Chemical shifts are reported in parts per million (ppm) and are referenced to internal tetramethylsilane ( $^1H$ ). Powder X-ray diffraction (PXRD) patterns were recorded with a Bruker D8 advance diffractometer equipped with nickel-filtered  $Cu-K_{\alpha}$  radiation. The powder X-ray diffraction (PXRD) patterns of complexes **1–4** are in good agreement with the simulated patterns (see Figures S11–S14 in the Supporting Information). The difference in intensities could be due to the preferred orientation in the powder samples.

**Magnetic Measurements:** Magnetic measurements on all samples were carried out with a Quantum Design MPMS 5S SQUID magnetometer in the temperature range 2–300 K. The measurements were performed on polycrystalline samples isolated from crystallization medium just before SQUID studies. The crystalline powders were mixed with grease and placed in gelatine capsules. The magnetic susceptibilities were measured in an applied field of 1 kOe. The molar susceptibilities ( $\chi_M$ ) were corrected for the sample holder, grease, and for the diamagnetic contributions of all atoms by using Pascal's tables.<sup>[25]</sup> Field-dependence magnetizations have been recorded at 2 K. The ac susceptibilities were collected for  $H_{AC} = 3$  Oe and frequencies up to 1500 Hz. All data are plotted for a  $Ln_4$  molecular complex.

**X-ray Crystallography:** The crystal data of all the compounds were collected with a Bruker SMART CCD diffractometer ( $Mo-K_{\alpha}$  radiation,  $\lambda = 0.71073$  Å). The SMART<sup>[26]</sup> program was used to collect frames of data, indexing reflections, and determining lattice parameters, SAINT<sup>[26]</sup> for integration of the intensities of reflections and scaling, SADABS<sup>[27]</sup> for absorption correction, and SHELXTL<sup>[28]</sup> for space-group determination and least-squares refinements on  $F^2$ . Structure solution and refinement were performed by using the SHELXT and SHELXL-2014/7 programs in the WinGX software package.<sup>[29]</sup> The best-fit models for the data sets were satisfactorily good. In spite of our best efforts to obtain the best quality data, several atoms in each of the structures incorporate thermal disorder, especially the phenyl and pyridyl rings, and the terminal  $CH_2OH$  and methyl groups in the main residues. In addition to these, the interstitial solvent molecules are highly disordered. Hence, we employed several restraints/constraints to achieve refinement stability. In the cases of very large thermal displacements, we partitioned the electron densities of the corresponding atoms into two positions and some of these atoms were refined isotropically. We could not assign

all the interstitial solvent molecules due to high disorder and weak residual Q peaks and hence they were squeezed out with the help of the PLATON/SQUEEZE program.<sup>[30]</sup> The void volumes and the possible squeezed out electron counts have been included in the corresponding CIFs. The treatment of disorder and refinement of the structures as well as the plausible origins of the alerts in the checkCIFs of the complexes are described in detail in the Supporting Information. The CIFs of all the complexes are provided in the Supporting Information. Crystal data and refinement parameters are summarized in Table 3. The ORTEP diagrams of complexes **1–4** are portrayed in Figure 2 and Figures S4–S6. In the case of the positionally disordered solvents/main residue atoms partitioned at two or three positions, only the positions of highest occupancy are shown in the ORTEP diagrams for clarity (Figure 2, a and Figures S4–S6).

CCDC 1457003 (for **1**), 1457004 (for **2**), 1457005 (for **3**) and 1457006 (for **4**) contain the supplementary crystallographic data for this paper. These data can be obtained free of charge from The Cambridge Crystallographic Data Centre.

**(E)-N'-(2-Hydroxy-3-(hydroxymethyl)-5-methylbenzylidene)-6-(hydroxymethyl)picolinohydrazide (LH<sub>4</sub>):** An ethanolic solution of 6-formyl-2-(hydroxymethyl)-4-methylphenol (1.10 g, 6.56 mmol) was added dropwise to a stirred solution of 6-(hydroxymethyl)picolinohydrazide (1.09 g, 6.56 mmol) in ethanol (60 mL) and the resulting solution was heated at reflux for 4 h. Then the solution was concentrated in vacuo to 20 mL and kept in a refrigerator at 0 °C overnight. A white precipitate was obtained that was filtered, washed with cold ethanol and diethyl ether, and dried, yield 1.61 g (76.92 %), m.p. 138 °C. FTIR (KBr):  $\tilde{\nu}$  = 3336 (br), 3206 (br), 3054 (m), 2918 (m), 2873 (m), 1666 (s), 1587 (s), 1539 (s), 1477 (w), 1429 (w), 1372 (w), 1339 (w), 1293 (w) cm<sup>-1</sup>. <sup>1</sup>H NMR (500 MHz, CD<sub>3</sub>OD):  $\delta$  = 2.34 (s, 3 H, Ar-Me), 4.60 (s, 2 H, Py-CH<sub>2</sub>OH), 4.81 (s, 2 H, Ar-CH<sub>2</sub>OH), 7.09 (s, 1 H, Ar-H), 7.26 (s, 1 H, Ar-H), 7.63 (d, 1 H, Py-H), 7.98 (t, 1

H, Py-H), 8.08 (d, 1 H, Py-H), 8.56 (s, 1 H, imino-H) ppm. C<sub>16</sub>H<sub>17</sub>N<sub>3</sub>O<sub>4</sub> (315.33): calcd. C 60.94, H 5.43, N 13.33; found C 61.57, H 5.77, N 12.10. MS (ESI): *m/z* = 316.12 [M + H]<sup>+</sup>.

**General Synthetic Procedure for the Preparation of the Complexes 1–4:** All the metal complexes **1–4** were prepared by following the same procedure as outlined here. Ln(NO<sub>3</sub>)<sub>3</sub>·5H<sub>2</sub>O (0.13 mmol) was added to a stirring solution of LH<sub>4</sub> (0.041 g, 0.13 mmol) in methanol (10 mL) to form an intense yellow solution. After 15 min of stirring at room temperature, triethylamine (0.051 mL, 0.39 mmol) was added dropwise and the resulting solution was stirred for a further 12 h at room temperature. Then the solution was filtered and kept for crystallization. Slow evaporation of the mother liquor for about 9 d led to yellow crystals that were suitable for X-ray diffraction. Specific details of each reaction and the characterization data of the complexes obtained are given below.

**[Dy<sub>4</sub>(LH<sub>2</sub>)<sub>4</sub>(μ<sub>2</sub>-OH)<sub>4</sub>]·4CH<sub>3</sub>OH·4H<sub>2</sub>O (**1**):** Quantities: LH<sub>4</sub> (0.041 g, 0.13 mmol), Dy(NO<sub>3</sub>)<sub>3</sub>·5H<sub>2</sub>O (0.057 g, 0.13 mmol), Et<sub>3</sub>N (0.051 mL, 0.39 mmol), yield 0.038 g, 51.47 % (based on Dy<sup>3+</sup>), m.p. 200 °C (decomp.). IR (KBr):  $\tilde{\nu}$  = 3387 (br), 2923 (w), 1616 (s), 1596 (s), 1564 (s), 1445 (w), 1384 (s), 1354 (s), 1263 (m), 1224 (m), 1185 (m), 1051 (w), 1015 (w), 849 (w), 818 (m), 757 (w) cm<sup>-1</sup>. MS (ESI): *m/z* = 1000.60 [C<sub>64</sub>H<sub>62</sub>Dy<sub>4</sub>N<sub>12</sub>O<sub>18</sub> + 2MeOH]<sup>2+</sup>. C<sub>70</sub>H<sub>100</sub>Dy<sub>4</sub>N<sub>12</sub>O<sub>32</sub> (**1**·4CH<sub>3</sub>OH·4H<sub>2</sub>O; 2271.6): calcd. C 37.01, H 4.44, N 7.4; found C 37.05, H 3.98, N 7.61.

**[Tb<sub>4</sub>(LH<sub>2</sub>)<sub>4</sub>(μ<sub>2</sub>-OH)<sub>4</sub>]·7CH<sub>3</sub>OH·3H<sub>2</sub>O (**2**):** Quantities: LH<sub>4</sub> (0.041 g, 0.13 mmol), Tb(NO<sub>3</sub>)<sub>3</sub>·5H<sub>2</sub>O (0.056 g, 0.13 mmol), Et<sub>3</sub>N (0.051 mL, 0.39 mmol), yield 0.032 g, 44.05 % (based on Tb<sup>3+</sup>), m.p. 200 °C (decomp.). IR (KBr):  $\tilde{\nu}$  = 3391 (br), 2936 (w), 1616 (s), 1595 (s), 1564 (w), 1443 (m), 1384 (m), 1354 (s), 1263 (w), 1225 (w), 1184 (w), 1050 (w), 1015 (w), 868 (w), 848 (m), 757 (w) cm<sup>-1</sup>. MS (ESI): *m/z* = 979.07 [C<sub>64</sub>H<sub>62</sub>Tb<sub>4</sub>N<sub>12</sub>O<sub>18</sub> + 2H<sub>2</sub>O]<sup>2+</sup>. C<sub>71</sub>H<sub>98</sub>N<sub>12</sub>O<sub>30</sub>Tb<sub>4</sub> ([Tb<sub>4</sub>(LH<sub>2</sub>)<sub>4</sub>(μ<sub>2</sub>-OH)<sub>4</sub>]·7CH<sub>3</sub>OH·3H<sub>2</sub>O; 2235.3): calcd. C 38.15, H 4.42, N 7.52; found C 38.13, H 3.79, N 7.63.

Table 3. Crystal data and structure refinement parameters of **1–4**.

	<b>1</b>	<b>2</b>	<b>3</b>	<b>4</b>
Formula	C <sub>66</sub> H <sub>55</sub> Dy <sub>4</sub> N <sub>12</sub> O <sub>24</sub>	C <sub>68</sub> H <sub>53</sub> N <sub>12</sub> O <sub>29</sub> Tb <sub>4</sub>	C <sub>64</sub> H <sub>55</sub> Ho <sub>4</sub> N <sub>12</sub> O <sub>33</sub>	C <sub>66</sub> H <sub>56</sub> Er <sub>4</sub> N <sub>12</sub> O <sub>27</sub>
<i>M</i> [g mol <sup>-1</sup> ]	2050.22	2137.95	2179.92	2118.27
Crystal system	triclinic	triclinic	triclinic	triclinic
Space group	<i>P</i> 	<i>P</i> 	<i>P</i> 	<i>P</i> 
<i>a</i> [Å]	14.131(5)	13.677(5)	14.108(5)	13.971(5)
<i>b</i> [Å]	15.962(5)	15.956(5)	16.007(5)	16.142(5)
<i>c</i> [Å]	19.114(5)	19.067(5)	18.684(5)	18.797(5)
$\alpha$ [°]	75.690(5)	79.247(5)	76.376(5)	75.333(5)
$\beta$ [°]	79.916(5)	77.702(5)	80.418(5)	81.295(5)
$\gamma$ [°]	88.508(5)	89.830(5)	89.088(5)	89.067(5)
<i>V</i> [Å <sup>3</sup> ]	4112(2)	3991(2)	4042(2)	4053(2)
<i>Z</i>	2	2	2	2
$\rho$ calcd. [g cm <sup>-3</sup> ]	1.656	1.725	1.791	1.736
$\mu$ [mm <sup>-1</sup> ]	3.667	3.48	3.962	4.180
<i>F</i> (000)	1982	2074	2110	2048
Crystal size [mm <sup>3</sup> ]	0.061 × 0.023 × 0.02	0.08 × 0.04 × 0.01	0.12 × 0.07 × 0.059	0.07 × 0.03 × 0.02
$\theta$ range [°]	1.9 to 28.32	2.01 to 24.88	4.08 to 25.02	1.9 to 28.4
Limiting indices	-18 ≤ <i>h</i> ≤ 18 -20 ≤ <i>k</i> ≤ 21 -25 ≤ <i>l</i> ≤ 24	-13 ≤ <i>h</i> ≤ 16 -18 ≤ <i>k</i> ≤ 18 -20 ≤ <i>l</i> ≤ 22	-16 ≤ <i>h</i> ≤ 16 -19 ≤ <i>k</i> ≤ 18 -17 ≤ <i>l</i> ≤ 22	-18 ≤ <i>h</i> ≤ 18 -21 ≤ <i>k</i> ≤ 21 -25 ≤ <i>l</i> ≤ 25
Reflns. collected	34017	81049	20950	61397
Independent reflns.	20297 [ <i>R</i> (int) = 0.0526]	14282 [ <i>R</i> (int) = 0.021]	13942 [ <i>R</i> (int) = 0.0418]	14230 [ <i>R</i> (int) = 0.0819]
Completeness to $\theta$ [%]	99	99.7	97.6	99.7
Refinement method			full-matrix least-squares on <i>F</i> <sup>2</sup>	
Goodness-of-fit on <i>F</i> <sup>2</sup>	0.86	0.859	1.059	0.95
Final <i>R</i> <sup>a,b</sup> indices	<i>R</i> <sub>1</sub> = 0.0695 <i>wR</i> <sub>2</sub> = 0.1830	<i>R</i> <sub>1</sub> = 0.0532 <i>wR</i> <sub>2</sub> = 0.1427	<i>R</i> <sub>1</sub> = 0.0615 <i>wR</i> <sub>2</sub> = 0.1685	<i>R</i> <sub>1</sub> = 0.0792 <i>wR</i> <sub>2</sub> = 0.1853

[a]  $R_1 = \sum |F_o - F_c| / \sum |F_o|$ . [b]  $wR_2 = \{[\sum w(F_o^2 - F_c^2)^2] / [\sum w(F_o^2)]\}^{1/2}$ .

**[Ho<sub>4</sub>(LH<sub>2</sub>)<sub>4</sub>(μ<sub>2</sub>-OH)<sub>4</sub>]·MeOH·8H<sub>2</sub>O (3):** Quantities: LH<sub>4</sub> (0.041 g, 0.13 mmol), Ho(NO<sub>3</sub>)<sub>3</sub>·5H<sub>2</sub>O (0.053 g, 0.13 mmol), Et<sub>3</sub>N (0.051 mL, 0.39 mmol), yield 0.04 g, 57.06 % (based on Ho<sup>3+</sup>), m.p. 200 °C (decomp.). IR (KBr):  $\tilde{\nu}$  = 3388 (br), 2938 (w), 1617 (s), 1590 (s), 1561 (w), 1443 (m), 1385 (m), 1354 (s), 1259 (w), 1224 (w), 1184 (w), 1050 (w), 1012 (w), 867 (w), 848 (m), 755 (w) cm<sup>-1</sup>. MS (ESI): *m/z* = 996.08 [C<sub>64</sub>H<sub>62</sub>Ho<sub>4</sub>N<sub>12</sub>O<sub>18</sub> + H<sub>2</sub>O + MeOH]<sup>2+</sup>. C<sub>65</sub>H<sub>84</sub>Ho<sub>4</sub>N<sub>12</sub>O<sub>29</sub> ([Ho<sub>4</sub>(LH<sub>2</sub>)<sub>4</sub>(μ<sub>2</sub>-OH)<sub>4</sub>]·CH<sub>3</sub>OH·8H<sub>2</sub>O; 2157.15): calcd. C 36.19, H 3.92, N 7.79; found C 36.01, H 3.47, N 7.97.

**[Er<sub>4</sub>(LH<sub>2</sub>)<sub>4</sub>(μ<sub>2</sub>-OH)<sub>4</sub>]·4CH<sub>3</sub>OH·5H<sub>2</sub>O (4):** Quantities: LH<sub>4</sub> (0.041 g, 0.13 mmol), Ho(NO<sub>3</sub>)<sub>3</sub>·5H<sub>2</sub>O (0.057 g, 0.13 mmol), Et<sub>3</sub>N (0.051 mL, 0.39 mmol), yield 0.042 g, 58.51 % (based on Er<sup>3+</sup>), m.p. 200 °C (decomp.). IR (KBr):  $\tilde{\nu}$  = 3388 (br), 2921 (w), 1617 (s), 1597 (s), 1546 (w), 1445 (m), 1384 (m), 1355 (s), 1263 (w), 1224 (w), 1186 (w), 1050 (w), 1016 (w), 869 (w), 850 (m), 757 (w) cm<sup>-1</sup>. MS (ESI): *m/z* = 1010.10 [C<sub>64</sub>H<sub>62</sub>Er<sub>4</sub>N<sub>12</sub>O<sub>18</sub> + 2MeOH]<sup>2+</sup>. C<sub>68</sub>H<sub>90</sub>Er<sub>4</sub>N<sub>12</sub>O<sub>29</sub> ([Er<sub>4</sub>(LH<sub>2</sub>)<sub>4</sub>(μ<sub>2</sub>-OH)<sub>4</sub>]·4CH<sub>3</sub>OH·5H<sub>2</sub>O; 2208.54): calcd. C 36.98, H 4.11, N 7.61; found C 37.01, H 3.97, N 7.84.

## Acknowledgments

The authors are thankful to the Department of Science and Technology (DST), New Delhi, for financial support, V. C. is thankful for a J. C. Bose National Fellowship. DST is also thanked for support through the Single-Crystal CCD X-ray Diffractometer facility at IIT-Kanpur. S. B. and S. D. thank the Council of Scientific and Industrial Research (CSIR), India for a Senior Research Fellowship. A. K. B. and J.-P. S. acknowledge the Indo-French Center for the Promotion of Advanced Research (CEFIPRA/IFCPAR) for support.

**Keywords:** Lanthanides · Single-molecule magnets · Magnetic properties · Quantum tunneling

- [1] a) R. Sessoli, H. L. Tsai, A. R. Schake, S. Wang, J. B. Vincent, K. Folting, D. Gatteschi, G. Christou, D. N. Hendrickson, *J. Am. Chem. Soc.* **1993**, *115*, 1804–1816; b) R. Sessoli, D. Gatteschi, D. Caneschi, M. A. Novak, *Nature* **1993**, *361*, 365.
- [2] a) A. Ardavan, S. J. Blundell, *J. Mater. Chem.* **2009**, *19*, 1754–1760; b) F. Troiani, M. Affronte, *Chem. Soc. Rev.* **2011**, *40*, 3119–3129; c) P. C. E. Stamp, A. Gaita-Ariño, *J. Mater. Chem.* **2009**, *19*, 1718–1730; d) J. Lehmann, A. Gaita-Ariño, E. Coronado, D. Loss, *Nat. Nanotechnol.* **2007**, *2*, 312–317; e) M. N. Leuenberger, D. Loss, *Nature* **2001**, *410*, 789–793.
- [3] a) M. Mannini, F. Pineider, C. Danieli, F. Totti, L. Sorace, P. Sainctavit, M. A. Arrio, E. Otero, L. Joly, J. C. Cezar, A. Cornia, R. Sessoli, *Nature* **2010**, *467*, 421; b) M. Gonidec, R. Biagi, V. Corradini, F. Moro, V. De Renzi, U. del Pennino, D. Summa, L. Muccioli, C. Zannoni, D. B. Amabilino, J. Veciana, *J. Am. Chem. Soc.* **2011**, *133*, 6603–6612; c) M. Urdampilleta, S. Klyatskaya, J.-P. Cleuziou, M. Ruben, W. Wernsdorfer, *Nat. Mater.* **2011**, *10*, 502–506; d) A. Candini, S. Klyatskaya, M. Ruben, W. Wernsdorfer, M. Affronte, *Nano Lett.* **2011**, *11*, 2634–2639.
- [4] a) M. Affronte, *J. Mater. Chem.* **2009**, *19*, 1731–1737; b) A. R. Rocha, V. M. García-Suárez, S. W. Bailey, C. J. Lambert, J. Ferrerand, S. Sanvito, *Nat. Mater.* **2005**, *4*, 335–339.
- [5] a) L. Bogani, W. Wernsdorfer, *Nat. Mater.* **2008**, *7*, 179–186; b) Y. Z. Zheng, M. Evangelisti, R. E. Winpenny, *Angew. Chem. Int. Ed.* **2011**, *50*, 3692–3695; *Angew. Chem.* **2011**, *123*, 3776; c) Y. Z. Zheng, M. Evangelisti, F. Tuna, R. E. Winpenny, *J. Am. Chem. Soc.* **2012**, *134*, 1057–1065; d) Y.-Z. Zheng, M. Evangelisti, R. E. P. Winpenny, *Chem. Sci.* **2011**, *2*, 99–102; e) W. Sethi, S. Sanz, K. S. Pedersen, M. A. Sorensen, G. S. Nichol, G. Lorusso, M. Evangelisti, E. K. Brechin, S. Piligkos, *Dalton Trans.* **2015**, *44*, 10315–10320; f) Y. Z. Zheng, G. J. Zhou, Z. Zheng, R. E. Winpenny, *Chem. Soc. Rev.* **2014**, *43*, 1462–1475; g) E. Colacio, J. Ruiz, G. Lorusso, E. K. Brechin, M. Evangelisti, *Chem. Commun.* **2013**, *49*, 3845–3847.
- [6] D. Gatteschi, R. Sessoli, *Angew. Chem. Int. Ed.* **2003**, *42*, 268–297; *Angew. Chem.* **2003**, *115*, 278.
- [7] a) T. Glaser, *Chem. Commun.* **2011**, *47*, 116–130; b) R. Inglis, L. F. Jones, G. Karotsis, A. Collins, S. Parsons, S. P. Perlepes, W. Wernsdorfer, E. K. Brechin, *Chem. Commun.* **2008**, 5924–5926; c) D. W. Boukhvalov, V. V. Dobrovitski, P. Kogerler, M. Al-Saqr, M. I. Katsnelson, A. I. Lichtenstein, B. N. Harmon, *Inorg. Chem.* **2010**, *49*, 10902–10906; d) H. Xu, Q. Wang, J.-H. Qin, S.-Q. Zang, S. K. Langley, K. S. Murray, B. Moubaraki, S. R. Batten, T. C. W. Mak, *Chem. Commun.* **2015**, *51*, 12716–12719; e) J. Liu, M. Qu, R. Clerac, X. M. Zhang, *Chem. Commun.* **2015**, *51*, 7356–7359; f) W. Guo, J. Bacsa, J. van Leusen, K. P. Sullivan, H. Lv, P. Kogerler, C. L. Hill, *Inorg. Chem.* **2015**, *54*, 10604–10609; g) O. Botezat, J. van Leusen, V. Ch. Kravtsov, A. Ellern, P. Kogerler, S. G. Baca, *Dalton Trans.* **2015**, *44*, 20753–20762; h) A. K. Bar, C. Pichon, J.-P. Sutter, *Coord. Chem. Rev.* **2016**, *308*, 346–380.
- [8] a) S. Osa, T. Kido, N. Matsumoto, N. Re, A. Pochaba, J. Mrozniski, *J. Am. Chem. Soc.* **2004**, *126*, 420–421; b) G. P. Guedes, S. Soriano, L. A. Mercante, N. L. Speziali, M. A. Novak, M. Andruh, M. G. Vaz, *Inorg. Chem.* **2013**, *52*, 8309–8311; c) C. M. Zaleski, E. C. Depperman, J. W. Kampf, M. L. Kirk, V. L. Pecoraro, *Angew. Chem. Int. Ed.* **2004**, *43*, 3912–3914; *Angew. Chem.* **2004**, *116*, 4002; d) O. Iasco, G. Novitchi, E. Jeanneau, D. Luneau, *Inorg. Chem.* **2013**, *52*, 8723–8731; e) T. K. Prasad, M. V. Rajasekharan, J. P. Costes, *Angew. Chem. Int. Ed.* **2007**, *46*, 2851–2854; *Angew. Chem.* **2007**, *119*, 2909; f) S. M. Abtab, M. C. Majee, M. Maity, J. Titus, R. Boca, M. Chaudhury, *Inorg. Chem.* **2014**, *53*, 1295–1306; g) V. Chandrasekhar, S. Das, A. Dey, S. Hossain, S. Kundu, E. Colacio, *Eur. J. Inorg. Chem.* **2014**, 397–406; h) V. Chandrasekhar, S. Das, A. Dey, S. Hossain, F. Lloret, E. Pardo, *Eur. J. Inorg. Chem.* **2013**, *4506*–4514; i) V. Chandrasekhar, P. Bag, M. Speldrich, J. van Leusen, P. Kogerler, *Inorg. Chem.* **2013**, *52*, 5035–5044; j) A. Deb, T. B. Boron, M. Itou, Y. Sakurai, T. Mallah, V. L. Pecoraro, J. E. Penner-Hahn, *J. Am. Chem. Soc.* **2014**, *136*, 4889–4892; k) C. M. Zaleski, J. W. Kampf, T. Mallah, M. L. Kirk, V. L. Pecoraro, *Inorg. Chem.* **2007**, *46*, 1954–1956; l) V. Baskar, K. Gopal, M. Hellwell, F. Tuna, W. Wernsdorfer, R. E. P. Winpenny, *Dalton Trans.* **2010**, *39*, 4747–4750; m) V. Chandrasekhar, B. M. Pandian, R. Azhakar, J. J. Vittal, R. Clérac, *Inorg. Chem.* **2007**, *46*, 5140–5142; n) V. Chandrasekhar, B. M. Pandian, R. Boomishankar, A. Steiner, J. J. Vittal, A. Houri, R. Clérac, *Inorg. Chem.* **2008**, *47*, 4918–4929; o) V. Chandrasekhar, P. Bag, W. Kroener, K. Gieb, P. Müller, *Inorg. Chem.* **2013**, *52*, 13078–13086; p) A. Chakraborty, P. Bag, J. Goura, A. K. Bar, J.-P. Sutter, V. Chandrasekhar, *Cryst. Growth Des.* **2015**, *15*, 848–857; q) I. Oyarzabal, J. Ruiz, E. Ruiz, D. Aravena, J. M. Seco, E. Colacio, *Chem. Commun.* **2015**, *51*, 12353–12356; r) K. R. Vignesh, S. K. Langley, B. Moubaraki, K. S. Murray, G. Rajaraman, *Chem. Eur. J.* **2015**, *21*, 16364–16369.
- [9] a) J. J. Baldoví, S. Cardona-Serra, J. M. Clemente-Juan, E. Coronado, A. Gaita-Arino, A. Palii, *Inorg. Chem.* **2012**, *51*, 12565–12574; b) D. N. Woodruff, R. E. Winpenny, R. A. Layfield, *Chem. Rev.* **2013**, *113*, 5110–5148; c) R. A. Layfield, *Organometallics* **2014**, *33*, 1084–1099; d) S. Biswas, H. S. Jena, A. Adhikary, S. Konar, *Inorg. Chem.* **2014**, *53*, 3926–3928; e) S. Goswami, A. Adhikary, H. S. Jena, S. Konar, *Dalton Trans.* **2013**, *42*, 9813–9817; f) J. A. Sheikh, A. Adhikary, S. Konar, *New J. Chem.* **2014**, *38*, 3006–3014; g) A. K. Jami, V. Baskar, E. C. Sanudo, *Inorg. Chem.* **2013**, *52*, 2432–2438; h) V. Chandrasekhar, P. Bag, E. Colacio, *Inorg. Chem.* **2013**, *52*, 4562–4570; i) S. Das, A. Dey, S. Biswas, E. Colacio, V. Chandrasekhar, *Inorg. Chem.* **2014**, *53*, 3417–3426; j) S. Das, S. Hossain, A. Dey, S. Biswas, J. P. Sutter, V. Chandrasekhar, *Inorg. Chem.* **2014**, *53*, 5020–5028; k) Q.-W. Li, J.-L. Liu, J.-H. Jia, Y.-C. Chen, J. Liu, L.-F. Wang, M.-L. Tong, *Chem. Commun.* **2015**, *51*, 10291–10294; l) M. Yadav, A. Mondal, V. Mereacre, S. K. Jana, A. K. Powell, P. W. Roesky, *Inorg. Chem.* **2015**, *54*, 7846–7856; m) W. Cao, C. Gao, Y.-Q. Zhang, D. Qi, T. Liu, K. Wang, C. Duan, S. Gao, J. Jiang, *Chem. Sci.* **2015**, *6*, 5947–5954; n) S. Biswas, S. Das, J. van Leusen, P. Kogerler, V. Chandrasekhar, *Dalton Trans.* **2015**, *44*, 19282–19293; o) V. E. Campbell, H. Bolvin, E. Riviere, R. Guillot, W. Wernsdorfer, T. Mallah, *Inorg. Chem.* **2014**, *53*, 2598–2605; p) V. E. Campbell, R. Guillot, E. Riviere, P. T. Brun, W. Wernsdorfer, T. Mallah, *Inorg. Chem.* **2013**, *52*, 5194–5200; q) A. Upadhyay, S. K. Singh, C. Das, R. Mondol, S. K. Langley, K. S. Murray, G. Rajaraman, M. Shanmugam, *Chem. Commun.* **2014**, *50*, 8838–8841; r) C. Das, S. Vaidya, T. Gupta, J. M. Frost, M. Righi, E. K. Brechin, M. Affronte, G. Rajaraman, M. Shanmugam, *Chem. Eur. J.* **2015**, *21*, 15639–15650.
- [10] a) Y.-N. Guo, G.-F. Xu, P. Gamez, L. Zhao, S.-Y. Lin, R. Deng, J. Tang, H.-J. Zhang, *J. Am. Chem. Soc.* **2010**, *132*, 8538–8539; b) Y. N. Guo, G. F. Xu,

- W. Wernsdorfer, L. Ungur, Y. Guo, J. Tang, H. J. Zhang, L. F. Chibotaru, A. K. Powell, *J. Am. Chem. Soc.* **2011**, *133*, 11948–11951; c) S. Y. Lin, W. Wernsdorfer, L. Ungur, A. K. Powell, Y. N. Guo, J. Tang, L. Zhao, L. F. Chibotaru, H. J. Zhang, *Angew. Chem. Int. Ed.* **2012**, *51*, 12767–12771; *Angew. Chem.* **2012**, *124*, 12939; d) P. Zhang, L. Zhang, C. Wang, S. Xue, S. Y. Lin, J. Tang, *J. Am. Chem. Soc.* **2014**, *136*, 4484–4487; e) Y. N. Guo, L. Ungur, G. E. Granroth, A. K. Powell, C. Wu, S. E. Nagler, J. Tang, L. F. Chibotaru, D. Cui, *Sci. Rep.* **2014**, *4*, 5471; f) Y. N. Guo, G. F. Xu, Y. Guo, J. Tang, *Dalton Trans.* **2011**, *40*, 9953–9963; g) P. Zhang, L. Zhang, J. Tang, *Dalton Trans.* **2015**, *44*, 3923–3929; h) P. Zhang, Y.-N. Guo, J. Tang, *Coord. Chem. Rev.* **2013**, *257*, 1728–1763; i) L. Ungur, S.-Y. Lin, J. Tang, L. F. Chibotaru, *Chem. Soc. Rev.* **2014**, *43*, 6894–6905; j) S. T. Liddle, J. van Slageren, *Chem. Soc. Rev.* **2015**, *44*, 6655–6669; k) K. Liu, X. Zhang, X. Meng, W. Shi, P. Cheng, A. K. Powell, *Chem. Soc. Rev.* **2016**, ASAP, DOI: 10.1039/c1035cs00770d; l) H. Wang, B.-W. Wang, Y. Bian, S. Gao, J. Jiang, *Coord. Chem. Rev.* **2016**, *306*, 195–216; m) F. Habib, M. Murugesu, *Chem. Soc. Rev.* **2013**, *42*, 3278–3288; n) L. Sorace, C. Benelli, D. Gatteschi, *Chem. Soc. Rev.* **2011**, *40*, 3092–3104; o) S. Gómez-Coca, D. Aravena, R. Morales, E. Ruiz, *Coord. Chem. Rev.* **2015**, 289–290, 379–392; p) J. Dreiser, *J. Phys. Condens. Matter* **2015**, *27*, 183203–183223.
- [11] R. J. Blagg, L. Ungur, F. Tuna, J. Speak, P. Comar, D. Collison, W. Wernsdorfer, E. J. L. McInnes, L. F. Chibotaru, R. E. P. Winpenny, *Nat. Chem.* **2013**, *5*, 673–678.
- [12] R. J. Blagg, C. A. Muryn, E. J. McInnes, F. Tuna, R. E. Winpenny, *Angew. Chem. Int. Ed.* **2011**, *50*, 6530–6533; *Angew. Chem.* **2011**, *123*, 6660.
- [13] S. A. Sulway, R. A. Layfield, F. Tuna, W. Wernsdorfer, R. E. P. Winpenny, *Chem. Commun.* **2012**, *48*, 1508–1510.
- [14] S. Demir, J. M. Zadrozy, M. Nippe, J. R. Long, *J. Am. Chem. Soc.* **2012**, *134*, 18546–18549.
- [15] a) V. Chandrasekhar, B. M. Pandian, J. J. Vittal, R. Clérac, *Inorg. Chem.* **2009**, *48*, 1148–1157; b) V. Chandrasekhar, B. M. Pandian, R. Boomishankar, A. Steiner, R. Clérac, *Dalton Trans.* **2008**, 5143–5145; c) V. Chandrasekhar, T. Senapati, A. Dey, S. Das, M. Kalisz, R. Clérac, *Inorg. Chem.* **2012**, *51*, 2031–2038.
- [16] a) V. Chandrasekhar, S. Hossain, S. Das, S. Biswas, J. P. Sutter, *Inorg. Chem.* **2013**, *52*, 6346–6353; b) J. Goura, J. P. Walsh, F. Tuna, V. Chandrasekhar, *Inorg. Chem.* **2014**, *53*, 3385–3391.
- [17] V. Chandrasekhar, S. Das, A. Dey, S. Hossain, J. P. Sutter, *Inorg. Chem.* **2013**, *52*, 11956–11965.
- [18] S. Biswas, S. Das, J. van Leusen, P. Kögerler, V. Chandrasekhar, *Eur. J. Inorg. Chem.* **2014**, 4159–4167.
- [19] a) S. Xue, L. Zhao, Y.-N. Guo, P. Zhang, J. Tang, *Chem. Commun.* **2012**, *48*, 8946–8948; b) Y. N. Guo, X. H. Chen, S. Xue, J. Tang, *Inorg. Chem.* **2011**, *50*, 9705–9713; c) J. Wu, L. Zhao, M. Guo, J. Tang, *Chem. Commun.* **2015**, *51*, 17317–17320.
- [20] a) S. Xue, L. Zhao, Y. N. Guo, J. Tang, *Dalton Trans.* **2012**, *41*, 351–353; b) N. M. Randell, M. U. Anwar, M. W. Drover, L. N. Dawe, L. K. Thompson, *Inorg. Chem.* **2013**, *52*, 6731–6742; c) M. U. Anwar, L. K. Thompson, L. N. Dawe, F. Habib, M. Murugesu, *Chem. Commun.* **2012**, *48*, 4576–4578.
- [21] a) M. L. Kahn, J.-P. Sutter, S. Golhen, P. Guionneau, L. Ouahab, O. Kahn, D. Chasseau, *J. Am. Chem. Soc.* **2000**, *122*, 3413–3421; b) M. L. Kahn, R. Ballou, P. Porcher, O. Kahn, J.-P. Sutter, *Chem. Eur. J.* **2002**, *8*, 525–531.
- [22] a) E. Lucaccini, L. Sorace, M. Perfetti, J.-P. Costes, R. Sessoli, *Chem. Commun.* **2014**, *50*, 1648–1651; b) R. Marx, F. Moro, M. Dorfel, L. Ungur, M. Waters, S. D. Jiang, M. Orlita, J. Taylor, W. Frey, L. F. Chibotaru, J. van Slageren, *Chem. Sci.* **2014**, *5*, 3287–3293; c) Y. Rechkemmer, J. E. Fischer, R. Marx, M. Dorfel, P. Neugebauer, S. Horvath, M. Gysler, T. Brock-Nannestad, W. Frey, M. F. Reid, J. van Slageren, *J. Am. Chem. Soc.* **2015**, *137*, 13114–13120; d) E. Lucaccini, M. Briganti, M. Perfetti, L. Vendier, J. P. Costes, F. Totti, R. Sessoli, L. Sorace, *Chem. Eur. J.* **2016**, *22*, 5552–5562.
- [23] a) M. Holynska, R. Clerac, M. Rouzieres, *Chem. Eur. J.* **2015**, *21*, 13321–13329; b) M. Ren, Z. L. Xu, T. T. Wang, S. S. Bao, Z. H. Zheng, Z. C. Zhang, L. M. Zheng, *Dalton Trans.* **2016**, *45*, 690–695; c) M. M. Hänninen, A. J. Mota, D. Aravena, E. Ruiz, R. Sillanpää, A. Camon, M. Evangelisti, E. Colacic, *Chem. Eur. J.* **2014**, *20*, 8410–8420; d) P.-E. Car, M. Perfetti, M. Mannini, A. Favre, A. Caneschi, R. Sessoli, *Chem. Commun.* **2011**, *47*, 3751–3753; e) L. Zhang, J. Jung, P. Zhang, M. Guo, L. Zhao, J. Tang, B. Le Guennic, *Chem. Eur. J.* **2016**, *22*, 1392–1398; f) H. L. Gao, L. Jiang, S. Liu, H. Y. Shen, W. M. Wang, J. Z. Cui, *Dalton Trans.* **2016**, *45*, 253–264; g) J. Ruiz, A. J. Mota, A. Rodriguez-Dieguez, S. Titos, J. M. Herrera, E. Ruiz, E. Cremades, J. P. Costes, E. Colacic, *Chem. Commun.* **2012**, *48*, 7916–7918; h) M. Jeletic, P. H. Lin, J. J. Le Roy, I. Korobkov, S. I. Gorelsky, M. Murugesu, *J. Am. Chem. Soc.* **2011**, *133*, 19286–19289; i) M. Gregson, N. F. Chilton, A.-M. Ariciu, F. Tuna, I. F. Crowe, W. Lewis, A. J. Blake, D. Collison, E. J. L. McInnes, R. E. Winpenny, S. T. Liddle, *Chem. Sci.* **2016**, *7*, 155–165.
- [24] a) A. J. Hannaford, P. W. G. Smith, A. R. Tatchell, *Vogel's Textbook of Practical Organic Chemistry*, 5th ed. (Ed.: B. S. Furniss) ELBS and Longman, London, **1989**; b) D. B. G. Williams, M. Lawton, *J. Org. Chem.* **2010**, *75*, 8351–8354; c) X. Zeng, D. Coquière, A. Alenda, E. Garrier, T. Prangé, Y. Li, O. Renaud, I. Jabin, *Chem. Eur. J.* **2006**, *12*, 6393–6402.
- [25] O. Kahn, *Molecular Magnetism*, VCH, Weinheim, Germany, **1993**.
- [26] SMART & SAINT Software Reference manuals, version 6.45, Bruker Analytical X-ray Systems, Inc., Madison, WI, **2003**.
- [27] G. M. Sheldrick, SADABS, a software for empirical absorption correction, version 2.05, University of Göttingen, Germany, **2002**.
- [28] a) G. M. Sheldrick, SHELXTL, version 2014/7, <http://shelx.uni-ac.gwdg.de/SHELX/index.php>; b) G. M. Sheldrick, SHELXTL, version 6.12, Bruker AXS Inc., Madison, WI, **2001**.
- [29] SHELXTL, version 6.1, Reference Manual.
- [30] A. L. Spek, *Acta Crystallogr., Sect. C* **2015**, *71*, 9–18.

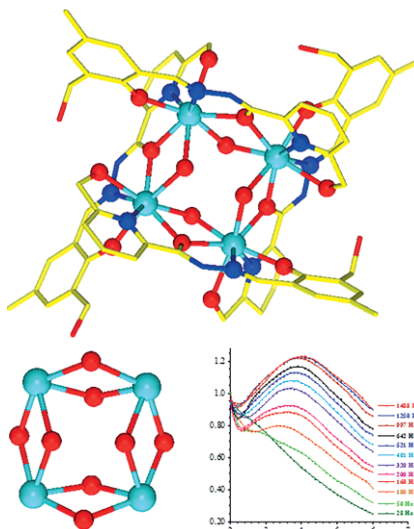
Received: July 11, 2016

Published Online: ■■■

**Lanthanide Square Grids**

S. Biswas, S. Das, S. Hossain,  
A. K. Bar, J.-P. Sutter,\*  
V. Chandrasekhar\* ..... 1–11

 **Tetranuclear Lanthanide(III) Complexes Containing a Square-Grid Core: Synthesis, Structure, and Magnetism**



The reactions of multidentate aryl hydrazone based ligands ( $LH_4$ ) with  $Ln(NO_3)_3$  in the presence of triethylamine has afforded a series of tetranuclear complexes  $[Ln_4(LH_2)_4(\mu_2-OH)_4] \cdot xCH_3OH \cdot yH_2O$  ( $Ln = Dy^{3+}$ ,  $x = 2$ ,  $y = 2$ ;  $Ln = Tb^{3+}$ ,  $x = 4$ ,  $y = 5$ ;  $Ln = Ho^{3+}$ ,  $x = 0$ ,  $y = 13$ ;  $Ln = Er^{3+}$ ,  $x = 4$ ,  $y = 6$ ). Detailed analysis of the magnetic data revealed that the  $Dy^{3+}$  analogue is a single-molecule magnet.

DOI: 10.1002/ejic.201600744